# Micropatterned Pyramidal Ionic Gels for Sensing Broad-Range Pressures with High Sensitivity

Sung Hwan Cho,[†] Seung Won Lee,[†] Seunggun Yu,[†] Hyeohn Kim,[†] Sooho Chang,[‡] Donyoung Kang,[‡] Ihn Hwang,[†] Han Sol Kang,[†] Beomjin Jeong,[†] Eui Hyuk Kim,[†] Suk Man Cho,[†] Kang Lib Kim,[†] Hyungsuk Lee,[‡] Wooyoung Shim,*,[†] and Cheolmin Park*,[†]

[†]Department of Materials Science and Engineering and [‡]School of Mechanical Engineering, Yonsei University Yonsei-ro 50, Seodaemun-gu, Seoul 03722, Republic of Korea

S Supporting Information
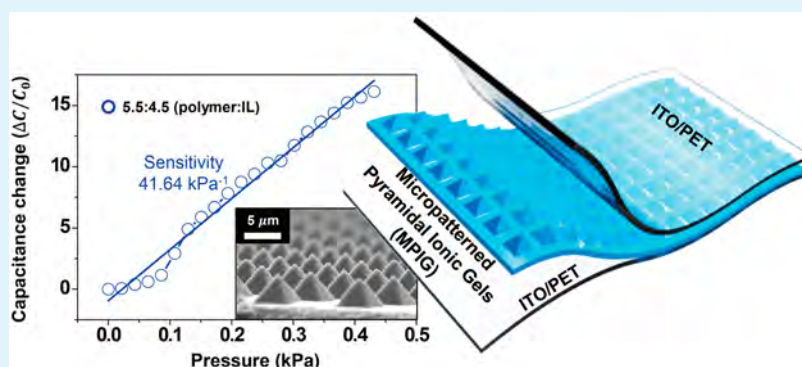
**ABSTRACT:** The development of pressure sensors that are effective over a broad range of pressures is crucial for the future development of electronic skin applicable to the detection of a wide pressure range from acoustic wave to dynamic human motion. Here, we present flexible capacitive pressure sensors that incorporate micropatterned pyramidal ionic gels to enable ultrasensitive pressure detection. Our devices show superior pressure-sensing performance, with a broad sensing range from a few pascals up to 50 kPa, with fast response times of <20 ms and a low operating voltage of 0.25 V. Since high-dielectric-constant ionic gels were employed as constituent sensing materials, an unprecedented sensitivity of 41 kPa$^{-1}$ in the low-pressure regime of <400 Pa could be realized in the context of a metal−insulator−metal platform. This broad-range capacitive pressure sensor allows for the efficient detection of pressure from a variety of sources, including sound waves, a lightweight object, jugular venous pulses, radial artery pulses, and human finger touch. This platform offers a simple, robust approach to low-cost, scalable device design, enabling practical applications of electronic skin.

**KEYWORDS:** capacitive pressure sensor, ionic polymer gels, topographical micropattern, arrays of periodic pyramids, high sensitivity, broad range pressure sensing, health monitoring

## INTRODUCTION

Pressure sensors have been of great interest in Internet of Things (IoTs) applications, including smart windows, displays, security systems, mobile phones, and prospective electronic skin (e-skin).[1−6] In particular, the ability to sense high pressures (>2 kPa) and low pressures (<30 Pa), e.g., blood pressure, human touch, and sound pulses, is significantly important for low-powered IoT sensors.[7−9] These pressure-sensing capabilities have been dramatically improved through the development of both resistive[10−18] and capacitive[19−33] sensing elements. The resistive sensors function based on electrical resistance changes upon pressure application; recently, 1-D or 2-D nanomaterials[10,12,14,15,17] with efficient network pressure-sensitive percolation have been used in high-sensitivity pressure sensors.[15,16] Significant advances in the development of resistive pressure sensors have enabled simple device construction and high pressure sensitivity. However, these sensors still suffer from

high power consumption much greater than that of capacitive pressure sensors for a voltage of ∼1 V.

Capacitive sensors utilize capacitance changes upon pressure application and are advantageous owing to their low power consumption, fast response times, and compact circuit layouts with vertically stacked device architectures.[19,21,23,26,28,31] The low pressure sensitivity of a capacitive sensor, however, is a disadvantage because most pressure-responsive materials such as elastomers and gels have low dielectric constants, which lead to low capacitance changes and therefore lower responsiveness to small pressure changes.[20,22,25−27] Sensors that adopt field effect transistor architectures show high sensitivity because small capacitance changes cause large alterations in the channel
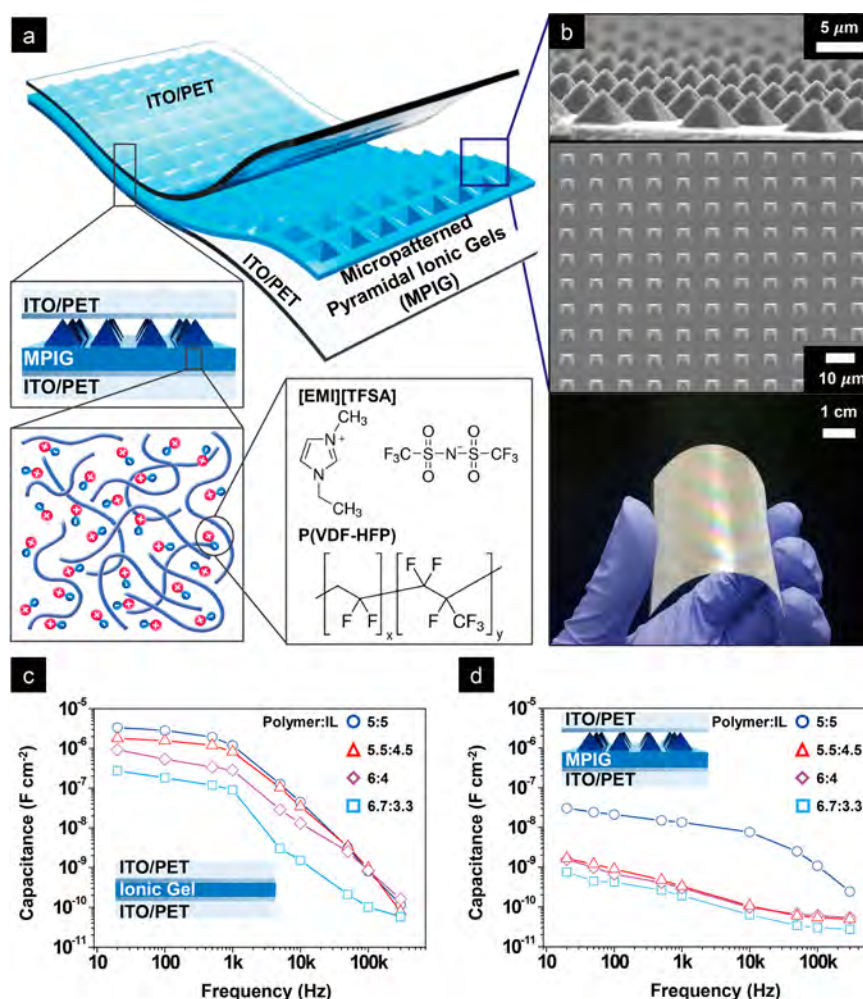
A

**Figure 1.** (a) Schematic illustration of a mechanically flexible capacitive type pressure sensor with an MPIG. The sensor consists of PET/ITO/MPIG/ITO/PET layers. The cross-sectional scheme of the sensor depicts the molecular structures of [EMI][TFSA] and P(VDF-HFP). (b) SEM images of the plane and inclined views of the arrays of pyramids periodically patterned with *p4mm* symmetry. Each pyramid is 5 $\mu$m in height. A photograph of an MPIG on ITO/PET over a large area ($8 \times 8$ cm$^2$). Capacitance of (c) PET/ITO/flat ionic gel/ITO and (d) ITO/MPIG/ITO with different ionic liquid (IL) contents as a function of frequency.

current, especially when a topographically micropatterned gate dielectric layer is used. However, the high driving voltage of ~50 V and complicated architecture, including a semiconducting channel and three terminal electrodes still remain a challenge.[21,31]

Ionic gels of polymer composites with ionic liquids (ILs), which have nonvolatile positive and negative charged ion pairs, exhibit high specific capacitances (>5 $\mu$F cm$^{-2}$) that arise from nanometer thick electrical double layers (EDLs) at the ionic liquid/electrode interfaces,[34−37] giving rise to pressure sensors with high sensitivity (~1 kPa$^{-1}$). For example, a poly(vinylidene fluoride-*co*-hexafluoropropylene), P(VDF-HFP), ionic gel has proven to be high capacitance gate dielectrics in a field effect transistor with high tensile strength characteristic, which provides an advantageous combination for pressure sensors. We envisioned that an ionic gel with a high dielectric constant could become more sensitive to pressure when it is topographically micropatterned. A topographically patterned ionic gel sandwiched between two electrodes contains periodic air gaps that are likely to decrease when pressurized, resulting in a dramatic increase in effective capacitance, even upon the application of small pressures.

We first present highly sensitive capacitive pressure sensors with topographically patterned arrays of pyramidal ionic gels,

positioned between two indium tin oxide (ITO) electrodes deposited on mechanically flexible poly(ethylene terephthalate) (PET) substrates. Micropatterned pyramidal ionic gels (MPIGs) exhibit significant capacitance variations as a function of pressure, resulting in unprecedented sensor sensitivities of ~41 kPa$^{-1}$ at pressures below 400 Pa and 13 kPa$^{-1}$ over the range between 0.5 and 5 kPa in the context of a metal−insulator−metal (MIM) platform. Our device is suitable for sensing a broad range of pressures up to 50 kPa, with a sensitivity greater than 2 kPa$^{-1}$, that allows for the efficient detection of pressure from a few pascals to tens of kilopascals, from a variety of sources including sound waves, a lightweight object, jugular venous pulses, radial artery pulses, and human (finger) touch.

## ■ EXPERIMENTAL SECTION

**Materials.** A thermoplastic copolymer (P(VDF-HFP)) with $M_n$ = 130 000 g mol$^{-1}$ and $M_w$ = 400 000 g mol$^{-1}$, 1-ethyl-3-methylimidazolium bis(trifluoromethylsulfonyl)amide ([EMI][TFSA]), acetone, indium tin oxide (ITO) coated on poly(ethylene terephthalate) (PET), and trichloro(*1H,1H,2H,2H*-perfluorooctyl)silane (FOTS) were purchased from Sigma-Aldrich and used as received.

**Fabrication of Capacitive Pressure Sensors.** A micropatterned pyramidal silicon mold was fabricated using a 4 in. (100) wafer with

300 nm thermally grown silicon oxide by photolithography, followed by chemical anisotropic etching using potassium hydroxide. Remaining silicon oxide was removed using buffered hydrofluoric acid. The arrays of engraved pyramids were developed in *p4mm* symmetry. Each pyramid had a square area of 5 × 5 $\mu$m and a height of 5 $\mu$m. The micropatterned Si mold was treated with $O_2$ plasma at 40 W for 3 min prior to the deposition of the FOTS self-assembled monolayer. A 15 wt % P(VDF-HFP) solution was prepared in acetone. Various amounts of [EMI][TFSA] were added to separate samples of this solution, followed by vigorous stirring at 75 °C for 30 min.[37] Four mixed solutions were prepared with P(VDF-HFP):IL weight ratio of 5:5, 5.5:4.5, 6:4, and 6.7:3.3 wt %. The IL/polymer solutions were then spin-coated onto micropatterned Si substrates at 1000 rpm and subsequently annealed at 75 °C for 24 h under $N_2$. The molded ionic gel films were peeled off from the Si molds and subsequently transferred onto ITO/PET substrates. Thickness of flat ionic gel and MPIG was 10 and 15 $\mu$m, respectively. Finally, the upper ITO/PET electrodes were carefully placed onto the MPIGs of the lower ITO/PET substrates (Figure S1, Supporting Information). Gold mesh was pasted on both ITO electrodes to ensure firm electrical contact for capacitance measurements. For monitoring jugular venous pulse and radial artery pulse pressures, 6 mm² sensors were prepared and attached onto the skin with a medical band.

**Measurement and Characterization.** The capacitance of an MPIG-containing pressure sensor was measured with a precision LCR (inductance, capacitance, resistance) meter (Agilent E4980A) under ambient conditions. The frequency was varied from 20 Hz to 300 kHz with an ac excitation voltage of 0.25 V. For pressure-dependent capacitance change measurements, a computer-controlled universal manipulator (Teraleader) was set up with the LCR meter. The vertical spatial and force resolutions of this equipment were 1 $\mu$m and 10 mN, respectively. To detect the variety of pressure sources including sound wave, a lightweight object, jugular venous pulses, radial artery pulses, and finger touch, the same LCR meter measurement setup was used without an additional amplification component. The transmittance of the MPIG-containing sensor was measured using a UV−vis−NIR spectrometer (Lambda 750, PerkinElmer). The thicknesses of the IL/polymer films were determined by a Dektak profiler. The microstructures of the MPIG were obtained using a field-emission scanning electron microscopy (FE-SEM, Model: JEOL 6701) with a 5 kV accelerating voltage.

**Effect of Pyramidal Patterns on Mechanical Responses.** A custom-made indenter, consisting of a load cell (GS0-10, Transducer Techniques), motorized stage (SM2-0803-3S and SZ-0604-3S, ST1), and a microscope camera (AM4113, AnMo Electronics Corporation), was used to probe the mechanical behavior of flat ion gels and MPIGs. Indentation experiments were performed by contacting a 1 mm diameter, stainless steel sphere, indentation tip with the sample. The maximum indentation depth was limited to 2 $\mu$m, and the indentation rate was 250 nm s$^{-1}$. Force and indentation depth curves were obtained as the tip approaches and retracts. The effective modulus of a sample was estimated from the force−indentation curve for tip approach, assuming Hertzian contact that follows $F = \frac{4}{3}\frac{E}{1-\nu^2}\sqrt{r}\,\delta^{3/2}$, where $F$, $E$, $\nu$, $r$, and $\delta$ are applied force, effective modulus, Poisson's ratio, radius of the indenter tip, and indentation depth, respectively. The Poisson's ratio of the ionic liquid gel was 0.5 assuming the ionic liquid gel is incompressible.[38] Attraction and adhesion forces between the tip and sample were characterized by the maximum negative force, in the force−indentation curve, obtained when the tip approaches and retracts, respectively.

## ■ RESULTS AND DISCUSSION

Our pressure sensor adopts a conventional capacitor structure, with pyramidal-shaped ionic gels (blue) and two ITO electrodes (gray) on PET (transparent) substrates (Figure 1a). The ionic gel was prepared using a blended solution of a P(VDF-HFP) as the structuring polymer and ([EMI][TFSA]) as the ionic liquid. The blended solution was then cast onto an anisotropically wet-etched silicon mold, giving rise to a film with arrays of pyramidal-shaped ion gel tips. The molded film was subsequently

transferred onto an ITO-deposited PET substrate, as shown in Figure 1a. We refer to these pyramidal-shaped dielectrics as MPIGs; they have several important features contributing to the highly sensitive, scalable, and flexible pressure sensors. First, each pyramidal tip has a square base with edges that are micrometers in length, tapering to a tip with a diameter of several hundreds of nanometers (top, Figure 1b), which decreases elastic resistance, in turn improving sensitivity to pressure. Second, this approach ensures high uniformity of the MPIG array over large areas, up to an entire 4 in. wafer (middle, Figure 1b, and Figure S1, Supporting Information). Third, by placing an MPIG on an ITO-deposited PET substrate, a mechanically flexible capacitive pressure sensor was fabricated over a large area of 8 × 8 cm² (bottom, Figure 1b). Note that light interference at the pyramidal-shaped tips results in a device transparency of approximately 40% (Figure S2).

We investigated the dielectric properties of P(VDF-HFP)-based topologically flat ion gels with MPIGs of differing ionic liquid content as a function of frequency. Unlike conventional low dielectric materials (i.e., polydimethylsiloxane rubber), these flat ion gels exhibit large specific capacitances (>1 $\mu$F cm$^{-2}$) that originate from the spontaneous formation of ion-pair EDLs upon application of the electric field, as shown in Figure 1c. When the polarity of the electric field is reversed, the ion pairs that were aligned along the previous field should rotate, giving rise to another set of EDLs of opposite polarity. This field-dependent rotation of the ionic liquid molecules creates two capacitors in series. Each capacitor has an extremely small charge separation distance, which is responsible for the large specific capacitance. In addition, at frequencies that are faster than the rotation speed of the ionic liquid molecules, EDLs were not effectively developed upon field reversal, giving rise to low capacitance. Indeed, in our flat ion gels, the capacitance abruptly decreases at a frequency of ~1 kHz, consistent with previous results.[28,36,37] The capacitance at a given frequency also increases with the ionic liquid content of the film.

On the other hand, the MPIG-containing capacitors show low specific capacitance values due to the large number of air gaps between the ITO electrodes, irrespective of the ionic liquid content of the MPIG, as shown in Figure 1d. While the observed specific capacitances of these MPIGs were below 0.1 $\mu$F cm$^{-2}$, the capacitances of MPIGs with 50 wt % ionic liquid are substantially higher than those with ionic liquid contents below 45 wt %; nevertheless, these values are still orders of magnitude lower than that of a flat ion gel, as shown in Figure 1c. The orders of magnitude difference in capacitance between a flat ion gel (i.e., zero air gap) and the MPIGs (the maximum air gap) implies that the capacitance with an MPIG depends significantly on the air gap fraction that can be readily controlled by applied pressure, making this capacitor highly sensitive to small pressures. A plot of $C_{\text{flat}}/C_{\text{pyramid}}$ ratios, based on Figures 1c and 1d, reveals that the largest difference in capacitance (~$10^3$), below 1 kHz, occurs with an ionic liquid content of 45 wt % (Figure S3), highlighting the potential use of these MPIG-incorporated pressure sensors. Given that small pressures are involved during the detection of blood pressure, human touch, and sound and that this pressure occurs mostly at the level of a few or tens of hertz,[7−9] our MPIGs will be useful in these fields.

Sensitivity, defined as $S = \delta(\Delta C/C_0)/\delta p$, where $p$ is the normal pressure and $C$ and $C_0$ are the capacitances with and without normal pressure, respectively, was measured for an MPIG capacitive pressure sensor with ionic liquid content of 45 wt % (Figure 2a). We evaluated the sensitivity by averaging individual
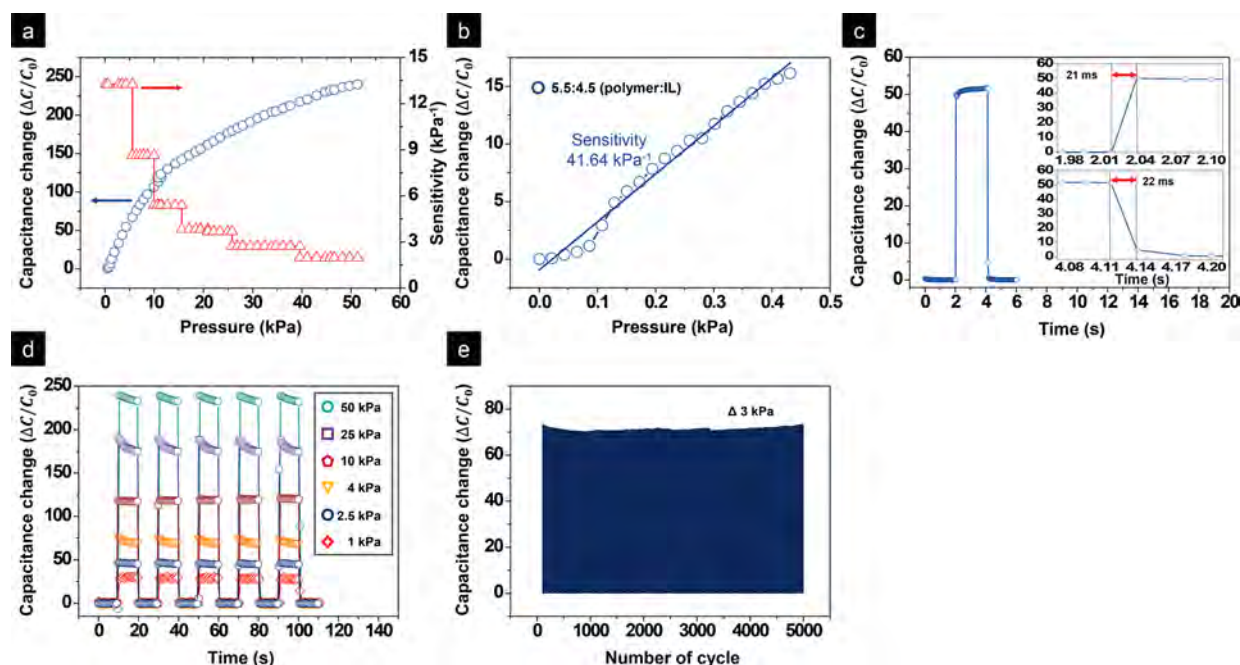
**Figure 2.** Pressure-sensing properties of an MPIG-containing capacitive sensor with a film composed of a 5.5:4.5 polymer/IL weight ratio. (a) Capacitance change ($\Delta C/C_0$) and sensitivity as a function of pressure. (b) A plot of the capacitance change as a function of pressure in the low, less than 400 Pa, pressure regime. (c) Time-resolved capacitance change response of an MPIG-containing pressure sensor at $\Delta$ 2.5 kPa. Both response and relaxation of the capacitance change occur within 20 ms, as shown in the inset. (d) Time-resolved capacitance change response of the sensor under repeated mechanical loads, with different pressures ranging from 1 to 50 kPa. (e) Endurance capacitance changes over 5000 cycles at $\Delta$ 3 kPa.

sensitivities at every 5 kPa pressure change. The results in Figure 2a (plot in red) show that the sensitivity is also pressure-dependent; a sensitivity of 13.2 kPa$^{-1}$ was obtained when the pressure was below 5 kPa, decreasing to 8.6 kPa$^{-1}$ up to 10 kPa, and 2 kPa$^{-1}$ at a pressure of 50 kPa. We note that sensitivity as a function of pressure decreases with increasing frequency, consistent with the decrease in MPIG capacitance at higher frequency, as observed in Figures 1c and 1d (Figure S4).

Great care should be taken when measuring the capacitance change at small pressures <500 Pa (near our measurement limit). Details of the experimental setup for pressure sensing below 500 Pa are shown in Figure S5. Briefly, for high applied pressure ranges (>500 Pa), the pressure sensor is firmly fixed to a glass slide using double-sided carbon tape, which guarantees firm contact between the pressing bar and the pressure sensor, without the possibility of slippage upon the application of pressure (Figure S5a). It should be noted that a carbon tape used to hold the sample does not affect the capacitance change upon pressure (Figure S6). For low-pressure ranges (<500 Pa), however, we manually raised the pressure by the incremental loading of unit glass slides (10 Pa, near the load limit of the instrument), while simultaneously recording changes in capacitance (Figure S5b). Note that the pressure was applied to the center of the sensor. Notably, the measured sensitivity in the low-pressure regime (~400 Pa) was approximately 41 kPa$^{-1}$, as shown in Figure 2b. For comparison, we prepared a sensor with a flat ionic gel and examined its sensitivity as a function of pressure. Negligible capacitance changes were observed in the low-pressure regime, and this varied slightly with increasing pressure, giving rise to a sensitivity value of approximately 0.01 kPa$^{-1}$ at high pressure (5 kPa) (Figure S7). The MPIGs are notably more sensitive, with sensitivity values ranging from 41 to 13 to 2 kPa$^{-1}$ at an applied pressure up to 50 kPa, and are to be compared with the state-of-the art results reported previously and plotted for comparison in

Figure S8 (see also Table S1). Pressure-sensing properties vary with the ionic liquid content of the MPIGs (Figure S9). In addition, there was not a significant dependence of sensing performance on the position of applied pressure (Figure S10).

Fast capacitance response and relaxation times upon the application of pressure should be guaranteed for high throughput sensing. Many pressure sensors use polymers as dielectric materials because they exhibit soft elastic deformation and recovery with changes in pressure, which leads to rapid increases and decays in capacitance, respectively. Our pyramidal arrays constructed from a pure P(VDF-HFP) film are glassy and barely responsive to small pressures but become mechanically elastic when ionic liquids are added. At high ionic liquid content, over 50 wt %, the arrays become viscoelastic and sticky and are not suitable for fast pressure sensing. A MPIG capacitive pressure sensor with an ionic liquid content of 45 wt %, however, is sufficiently elastic, leading to an instantaneous response in capacitance upon the application of pressure, as shown in Figures 2c and 2d. This ionic gel, which behaves as ionic conductor, has proven to have elastic properties with weak viscoelastic behavior as the content of ionic liquid decreases, as reported in previous study.[37] The rise and decay time required for complete capacitance change at 2.5 kPa pressure is approximately 20 ms, with negligible capacitance time lag. This fast response behavior can be attributed to the sharp end point of pyramidal geometry and may increase by decreasing the content of ionic liquids given that a lower content of ionic liquid yields lower viscoelasticity.[39] We note that this response time is comparable to those obtained from sensors containing polymer elastomers;[7−9] however, the sensitivities of our sensors are orders of magnitude higher than those of the reported sensors. In addition, fast responses were observed over the broad range of applied pressure (1−50 kPa), as shown in Figure 2d. In addition, our sensor endured 5000 loading−unloading cycles (1 s for loading and

unloading and 1s of intervals) at 3 kPa and maintained its function with minimal output signal degradation (Figure 2e), confirming that it is a highly robust MPIG-incorporated pressure sensor.

The unique mechanical properties of an MPIG were further elucidated by cyclic loading–unloading indentation experiments. Briefly, indentations were performed in a customized indenter with a ball tip of ~1 mm in diameter (Figure 3a). This tip was
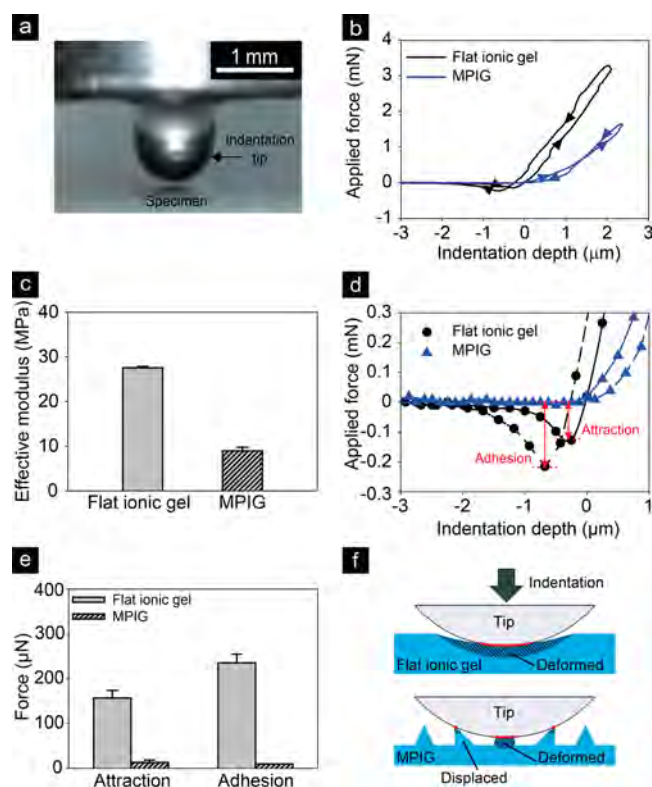


**Figure 3.** (a) Side view of the indentation experiment: indentation tip and ionic gel specimen. Scale bar: 1 mm. (b) Representative force–indentation curves for the flat ionic gel and the MPIG when a tip approaches and retracts. (c) Effective modulus of the flat ionic gel and the MPIG is estimated to be $28 \pm 0.3$ and $9 \pm 0.8$ MPa, respectively. (d) Attraction and adhesion are characterized by measuring the maximum negative force (red arrow) in the force–indentation curves for approach (solid line) and retraction (dotted line), respectively. (e) For the flat ionic gel, attraction and adhesion force are $157 \pm 17 \mu N$ and $235 \pm 20 \mu N$, respectively. In contrast, both forces are negligible and close to zero in the MPIG. (f) Schematic illustrations that demonstrate the effect of the pyramidal patterns on contact area (red line) and deformation region (dashed area) during indentation. When a tip makes contact with the MPIG, some pyramids undergo deformation and others undergo displacement. As a result, both contact and deformation areas can be reduced.

designed to be pressed to a depth of 2 $\mu$m into the surfaces of a flat ionic gel and an MPIG, with loading and unloading rates of 250 nm s$^{-1}$. First, to deform to this depth, a smaller force was required for the MPIG than was required for the flat ionic gel because the MPIG is highly compressible. The effective modulus, defined by applied force ($F$)–indentation depth ($d$) slope $F/d$, of the MPIG was 3 times smaller than that of the flat ionic gel (Figure 3b), at approximately 9 and 28 MPa, respectively (Figure 3c and Figure S11), indicating that MPIG is readily deformable. Second, the loading–unloading cycle for the flat ionic gel exhibited hysteresis between the loading and unloading paths, while there was a much smaller hysteresis for the MPIG,

originating from near elastic behavior that allows for fast response and relaxation. Third, the MPIG exhibited significantly lower attraction and adhesion forces over the flat ionic gel, as shown in Figure 3d. Indeed, we found that the attraction forces for the flat ionic gel and the MPIG were approximately 157 and 13 $\mu$N, respectively; similarly, the adhesion forces for these materials were 235 and 10 $\mu$N, respectively (Figure 3e). These results suggest that high sensitivity and repeatability, in the context of sensing performance, observed for the MPIG can be attributed to its low effective modulus, low attraction force, and low adhesion force, which lead to improved mechanical behavior. Consequently, micropyramidal patterns play key roles in reducing these properties by altering the mode of deformation (decreasing elastic resistance) and the contact area (decreasing adhered area), as shown schematically in Figure 3f.

Highly sensitive pressure sensors incorporating MPIG dielectrics allow us to efficiently detect a wide range of pressures in a single-device platform. For demonstration, we monitored the capacitance changes arising from a variety of pressure sources, including (i) sound from a commercial speaker (<30 Pa), (ii) a lightweight flower (4 Pa), (iii) jugular venous pulses (JVP) (2 kPa, $\approx\Delta$ 15 mmHg), (iv) radial artery pulses (4 kPa, $\approx\Delta$ 35 mmHg), (v) human finger touch (<10 kPa), and (vi) finger motion (<25 kPa). These pressure sources cover a range of generated pressures, from a few Pa to tens of kPa, as shown in Figure 4a and Figure S12. The results in Figure 4 clearly show that our device is capable of accurately detecting the various pressures described above. Specifically, the subtle variations in pressure, of the order of a few Pa, arising from sound pulses (80–100 dB) were successfully converted into capacitances, as shown in Figure 4b (see also Figure S13). In addition, a flower of approximately 40 mg in weight was successfully detected when placed on the surface of a sensor, as shown in Figure 4c (Figure S14). A JVP signal is composed of five component waves that include right atrial contraction (A), bulging of the tricuspid valve into the right atrium during ventricular systole (C), atrial relaxation and downward movement of the tricuspid valve (X), venous filling when the tricuspid valve is closed, and venous pressure increases from venous return (V) and blood filling into the right ventricle when the tricuspid valve opens (Y).[29] The characteristic JVP patterns for the A, C, X, V, and Y modes are clearly distinguishable, as shown in Figure 4d. Furthermore, characteristic radial artery pulses, $P_1$ and $P_2$, were visualized through capacitance changes (Figure 4e). From the $P_1$ and $P_2$ values in the inset of Figure 4e, we were able to determine the radial augmentation index ($AI_r = P_2/P_1$) and time delay between the first and second pressure peaks ($\Delta T_{DVP} = t_2 - t_1$).[21,29,33] For a 27 year old man, $AI_r$ and $\Delta T_{DVP}$ values of 0.76 and 149 ms, respectively, were obtained using our sensor. The values are typically observed for a healthy adult male and are consistent with those obtained by conventional pressure sensors.[40] Our MPIG sensor was also sensitive not only to finger touch, delivering from a few to approximately 10 kPa pressure, but also to compression arising from finger bending motion that corresponds to approximately tens of kPa, as shown in Figures 4f and 4g.

## ■ CONCLUSIONS

In summary, we demonstrated that ionic gels, composed of a blend of polymer and nonvolatile ionic liquid, are useful for sensing pressures over the broad range up to 50 kPa. These gels display high-pressure sensitivity when topographically patterned with arrays of periodic pyramids. Our capacitive pressure sensor exhibited sensitivities of 13 kPa$^{-1}$ at 5 kPa, 8.7 kPa$^{-1}$ at 10 kPa,
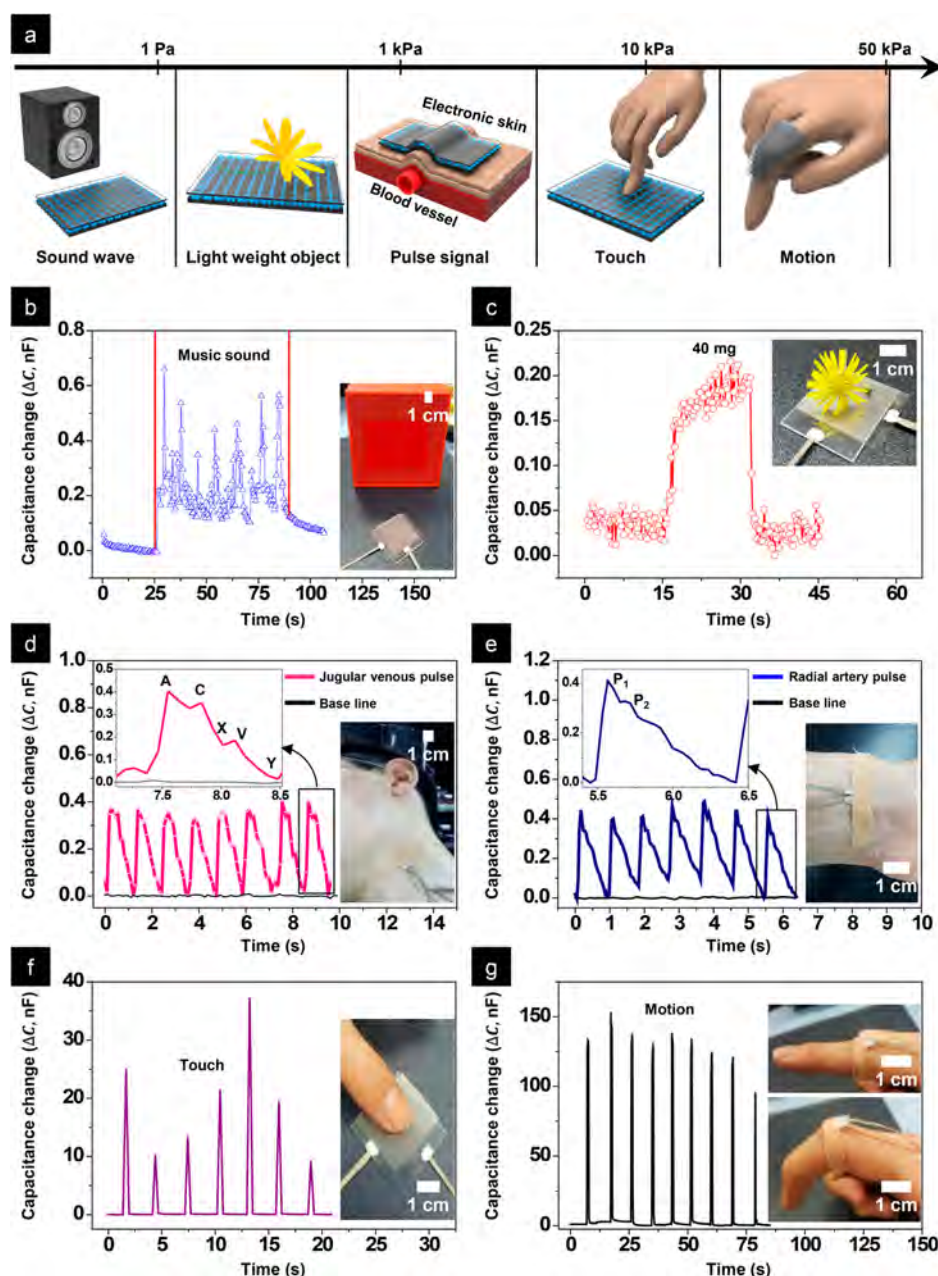
**Figure 4.** Broad range pressure sensing by an MPIG-containing sensor composed of a 5.5:4.5 polymer/IL ratio. (a) Schematic illustration of sensing over variety of pressure sources, from a few Pa to tens of kPa. (b) Response of the sensor to sound waves generated from a conventional speaker (inset). (c) Pressure response of the sensor to a lightweight flower (40 mg) placed on the top of the sensor (inset). (d) The measurement of jugular venous pulse patterns by the sensor attached onto middle of the neck using medical tape (inset). The magnified inset shows a typical jugular venous pulse with its five characteristic peaks. (e) The signal curves of a real-time pulse wave from the radial artery in the wrist. The inset shows a photograph of the sensor attached to the wrist with medical tape. The magnified singe radial pulse wave exhibits two characteristic peaks that correspond to the heartbeat and the reflected wave from hand. Real-time monitoring of capacitance changes from pressure arising from (f) a finger touching and (g) finger bending.

$5.2 \text{ kPa}^{-1}$ at 15 kPa, and approximately $2.1 \text{ kPa}^{-1}$ at 50 kPa. More interestingly, we elucidated a sensitivity of $41 \text{ kPa}^{-1}$ at a pressure of 400 Pa and below. In addition, the fast capacitance response to applied pressure and consistent device operation over multiple pressure cycles are attributed to the elastic properties of our MPIG that result from its low modulus, surface attraction, and adhesion properties. This approach, combined high capacitance dielectrics with robust mechanical strength, is not limited to P(VDF-HFP)-based ionic gels but can extend to other ionic gels with similar electrical and mechanical characteristics, which merits further study. Our reliable, low power, highly sensitive, and broad pressure range sensor was suitable for the efficient

detection of a variety of pressure sources arising from sound, a lightweight object, jugular venous pulses, radial artery pulses, finger touch, and finger motion.

## ■ ASSOCIATED CONTENT

### Ⓢ Supporting Information

The Supporting Information is available free of charge on the ACS Publications website at DOI: 10.1021/acsami.7b00398.

> Fabrication processes and transmittance of a pressure sensor, capacitance ratio of flat ionic gels to MPIGs, pressure sensing properties as a function of frequency and

IL content, measurement setup, pressure sensing properties of flat PDMS-based capacitive sensor and a flat ionic gel film, comparison of sensitivity values from our work with those of representative previous work, the position dependence of sensing performance, effective modulus, absolute values of capacitance change, pressure response of a sensor to music and the lightweight object, characteristics of the capacitive pressure sensors reported in the literature and the current work (PDF)

## ■ AUTHOR INFORMATION

**Corresponding Authors**
*E-mail wshim@yonsei.ac.kr; Ph +82-2-2123-2833; Fax +82-2-312-5375 (W.S.).
*E-mail cmpark@yonsei.ac.kr; Ph +82-2-2123-2833; Fax +82-2-312-5375 (C.P.).

**ORCID** 
Wooyoung Shim: 0000-0002-7601-6282
Cheolmin Park: 0000-0002-6832-0284

**Author Contributions**
S.H.C. and S.W.L. contributed equally to the work.

**Notes**
The authors declare no competing financial interest.

## ■ REFERENCES

(1) Morin, S. A.; Shepherd, R. F.; Kwok, S. W.; Stokes, A. A.; Nemiroski, A.; Whitesides, G. M. Camouflage and Display for Soft Machines. *Science* **2012**, *337*, 828−832.

(2) Wang, C.; Hwang, D.; Yu, Z.; Takei, K.; Park, J.; Chen, T.; Ma, B.; Javey, A. User-Interactive Electronic Skin for Instantaneous Pressure Visualization. *Nat. Mater.* **2013**, *12*, 899−904.

(3) Kim, S. H.; Hong, K.; Xie, W.; Lee, K. H.; Zhang, S.; Lodge, T. P.; Frisbie, C. D. Electrolyte-Gated Transistors for Organic and Printed Electronics. *Adv. Mater.* **2013**, *25*, 1822−1846.

(4) Wei, X. Y.; Wang, X.; Kuang, S. Y.; Su, L.; Li, H. Y.; Wang, Y.; Pan, C.; Wang, Z. L.; Zhu, G. Dynamic Triboelectrification-Induced Electroluminescence and its Use in Visualized Sensing. *Adv. Mater.* **2016**, *28*, 6656−6664.

(5) Cho, S. H.; Sung, J.; Hwang, I.; Kim, R. H.; Choi, Y. S.; Jo, S. S.; Lee, T.-W.; Park, C. High Performance AC Electroluminescence from Colloidal Quantum Dot Hybrids. *Adv. Mater.* **2012**, *24*, 4540−4546.

(6) Wang, J.; Yan, C.; Chee, K. J.; Lee, P. S. Highly Stretchable and Self-Deformable Alternating Current Electroluminescent Devices. *Adv. Mater.* **2015**, *27*, 2876−2882.

(7) Trung, T. Q.; Lee, N.-E. Flexible and Stretchable Physical Sensor Integrated Platforms for Wearable Human-Activity Monitoring and Personal Healthcare. *Adv. Mater.* **2016**, *28*, 4338−4372.

(8) Zang, Y.; Zhang, F.; Di, C.-A.; Zhu, D. Advances of Flexible Pressure Sensors toward Artificial Intelligence and Health Care Applications. *Mater. Horiz.* **2015**, *2*, 140−156.

(9) Chortos, A.; Liu, J.; Bao, Z. Pursuing Prosthetic Electronic Skin. *Nat. Mater.* **2016**, *15*, 937−950.

(10) You, I.; Kim, B.; Park, J.; Koh, K.; Shin, S.; Jung, S.; Jeong, U. Stretchable E-Skin Apexcardiogram Sensor. *Adv. Mater.* **2016**, *28*, 6359−6364.

(11) Yao, H.-B.; Ge, J.; Wang, C. F.; Wang, X.; Hu, Z.; Zheng, Z.-J.; Ni, Y.; Yu, S.-H. A Flexible and Highly Pressure-Sensitive Graphene-Polyurethane Sponge Based on Fractured Microstructure Design. *Adv. Mater.* **2013**, *25*, 6692−6698.

(12) Pan, L.; Chortos, A.; Yu, G.; Wang, Y.; Isaacson, S.; Allen, R.; Shi, Y.; Dauskardt, R.; Bao, Z. An Ultra-Sensitive Resistive Pressure Sensor Based on Hollow-Sphere Microstructure Induced Elasticity in Conducting Polymer Film. *Nat. Commun.* **2014**, *5*, 3002−3009.

(13) Pang, C.; Lee, G. Y.; Kim, T. I.; Kim, S. M.; Kim, H. N.; Ahn, S. H.; Suh, K. Y. A Flexible and Highly Sensitive Strain-Gauge Sensor Using Reversible Interlocking of Nanofibres. *Nat. Mater.* **2012**, *11*, 795−801.

(14) Lee, S.; Reuveny, A.; Reeder, J.; Lee, S.; Jin, H.; Liu, Q.; Yokota, T.; Sekitani, T.; Isoyama, T.; Abe, Y.; Suo, Z.; Someya, T. A Transparent Bending-Insensitive Pressure Sensor. *Nat. Nanotechnol.* **2016**, *11*, 472−478.

(15) Chen, Z.; Ming, T.; Goulamaly, M. M.; Yao, H.; Nezich, D.; Hempel, M.; Hofmann, M.; Kong, J. Enhancing the Sensitivity of Percolative Graphene Films for Flexible and Transparent Pressure Sensor Arrays. *Adv. Funct. Mater.* **2016**, *26*, 5061−5067.

(16) Gong, S.; Schwalb, W.; Wang, Y.; Chen, Y.; Tang, Y.; Si, J.; Shirinzadeh, B.; Cheng, W. A Wearable and Highly Sensitive Pressure Sensor with Ultrathin Gold Nanowires. *Nat. Commun.* **2014**, *5*, 3132−3139.

(17) Bae, G. Y.; Pak, S. W.; Kim, D.; Lee, G.; Kim, D. H.; Chung, Y.; Cho, K. Linearly and Highly Pressure-Sensitive Electronic Skin Based on a Bioinspired Hierarchical Structural Array. *Adv. Mater.* **2016**, *28*, 5300−5306.

(18) Ramuz, M.; Tee, B. C.-K.; Tok, J. B.-H.; Bao, Z. Transparent, Optical, Pressure-Sensitive Artificial Skin for Large-Area Stretchable Electronics. *Adv. Mater.* **2012**, *24*, 3223−3227.

(19) Mannsfeld, S. C. B.; Tee, B. C.-K.; Stoltenberg, R. M.; Chen, C. V. H-H.; Barman, S.; Muir, B. V. O.; Sokolov, A. N.; Reese, C.; Bao, Z. Highly Sensitive Flexible Pressure Sensors with Microstructured Rubber Dielectric Layers. *Nat. Mater.* **2010**, *9*, 859−864.

(20) Lipomi, D. J.; Vosgueritchian, M.; Tee, B. C.-K.; Hellstrom, S. L.; Lee, J. A.; Fox, C. H.; Bao, Z. Skin-Like Pressure and Strain Sensors Based on Transparent Elastic Films of Carbon Nanotubes. *Nat. Nanotechnol.* **2011**, *6*, 788−792.

(21) Schwartz, G.; Tee, B. C.-K.; Mei, J.; Appleton, A. L.; Kim, D. H.; Wang, H.; Bao, Z. Flexible Polymer Transistors with High Pressure Sensitivity for Application in Electronic Skin and Health Monitoring. *Nat. Commun.* **2013**, *4*, 1859−1866.

(22) Wang, X.; Li, T.; Adams, J.; Yang, J. Transparent, Stretchable, Carbon-Nanotube-Inlaid Conductors Enabled by Standard Replication Technology for Capacitive Pressure, Strain and Touch Sensors. *J. Mater. Chem. A* **2013**, *1*, 3580−3586.

(23) Tee, B. C.-K.; Chortos, A.; Dunn, R. R.; Schwartz, G.; Eason, E.; Bao, Z. Tunable Flexible Pressure Sensors using Microstructured Elastomer Geometries for Intuitive Electronics. *Adv. Funct. Mater.* **2014**, *24*, 5427−5434.

(24) Park, S.; Kim, H.; Vosgueritchian, M.; Cheon, S.; Kim, H.; Koo, J. H.; Kim, T. R.; Lee, S.; Schwartz, G.; Chang, H.; Bao, Z. Stretchable Energy-Harvesting Tactile Electronic Skin Capable of Differentiating Multiple Mechanical Stimuli Modes. *Adv. Mater.* **2014**, *26*, 7324−7332.

(25) Sun, J.-Y.; Keplinger, C.; Whitesides, G. M.; Suo, Z. Ionic Skin. *Adv. Mater.* **2014**, *26*, 7608−7614.

(26) Viry, L.; Levi, A.; Totaro, M.; Mondini, A.; Mattoli, V.; Mazzolai, B.; Beccai, L. Flexible Three-Axial Force Sensor for Soft and Highly Sensitive Artificial Touch. *Adv. Mater.* **2014**, *26*, 2659−2664.

(27) Lee, J.; Kwon, H.; Seo, J.; Shin, S.; Koo, J. H.; Pang, C.; Son, S.; Kim, J. H.; Jang, Y. H.; Kim, D. E.; Lee, T. Conductive Fiber-Based Ultrasensitive Textile Pressure Sensor for Wearable Electronics. *Adv. Mater.* **2015**, *27*, 2433−2439.

(28) Nie, B.; Li, R.; Cao, J.; Brandt, J. D.; Pan, T. Flexible Transparent Iontronic Film for Interfacial Capacitive Pressure Sensing. *Adv. Mater.* **2015**, *27*, 6055−6062.

(29) Pang, C.; Koo, J. H.; Nguyen, A.; Caves, J. M.; Kim, M.-G.; Chortos, A.; Kim, K.; Wang, P. J.; Tok, J. B.-H.; Bao, Z. Highly Skin-Conformal Microhairy Sensor for Pulse Signal Amplification. *Adv. Mater.* **2015**, *27*, 634−640.

(30) Wang, J.; Jiu, J.; Nogi, M.; Sugahara, T.; Nagao, S.; Koga, H.; He, P.; Suganuma, K. A Highly Sensitive and Flexible Pressure Sensor with Electrodes and Elastomeric Interlayer Containing Silver Nanowires. *Nanoscale* **2015**, *7*, 2926−2932.

(31) Zang, Y.; Zhang, F.; Huang, D.; Gao, X.; Di, C.-A.; Zhu, D. Flexible Suspended Gate Organic Thin-Film Transistors for Ultra-Sensitive Pressure Detection. *Nat. Commun.* **2015**, *6*, 6269−6277.

(32) Chen, Y.-M.; He, S.-M.; Huang, C. H.; Huang, C.-H.; Shih, W.-P.; Chu, C.-L.; Kong, J.; Li, J.; Su, C.-Y. Ultra-Large Suspended Graphene as a Highly Elastic Membrane for Capacitive Pressure Sensors. *Nanoscale* **2016**, *8*, 3555−3564.

(33) Gao, Y.; Song, J.; Li, S.; Elowsky, C.; Zhou, Y.; Ducharme, S.; Chen, Y. M.; Zhou, Q.; Tan, L. Hydrogel Microphones for Stealthy Underwater Listening. *Nat. Commun.* **2016**, *7*, 12316−12326.

(34) Keplinger, C.; Sun, J.-Y.; Foo, C. C.; Rothemund, P.; Whitesides, G. M.; Suo, Z. Stretchable, Transparent, Ionic Conductors. *Science* **2013**, *341*, 984−987.

(35) Nohara, S.; Wada, H.; Furukawa, N.; Inoue, H.; Morita, M.; Iwakura, C. Electrochemical Characterization of New Electric Double Layer Capacitor with Polymer Hydrogel Electrolyte. *Electrochim. Acta* **2003**, *48*, 749−753.

(36) Cho, J. H.; Lee, J.; Xia, Y.; Kim, B.; He, Y.; Renn, M. J.; Lodge, T. P.; Frisbie, C. D. Printable Ion-Gel Gate Dielectrics for Low-Voltage Polymer Thin-Film Transistors on Plastic. *Nat. Mater.* **2008**, *7*, 900−906.

(37) Lee, K. H.; Kang, M. S.; Zhang, S.; Gu, Y.; Lodge, T. P.; Frisbie, C. D. "Cut and Stick" Rubbery Ion Gels as High Capacitance Gate Dielectrics. *Adv. Mater.* **2012**, *24*, 4457−4462.

(38) Li, M.; Li, J.; Na, H.; Vlassak, J. J. Mechanical Behavior of Poly(methyl methacrylate)-Based Ionogels. *Soft Matter* **2014**, *10*, 7993−8000.

(39) Zhang, S. P.; Lee, K. H.; Frisbie, C. D.; Lodge, T. P. Ionic Conductivity, Capacitance, and Viscoelastic Properties of Block Copolymer-Based Ion Gels. *Macromolecules* **2011**, *44*, 940−949.

(40) Nichols, W. W. Clinical Measurement of Arterial Stiffness Obtained from Noninvasive Pressure Waveforms. *Am. J. Hypertens.* **2005**, *18*, 3−10.